Metamorphism and deformation in the El Fuerte region: their role in the tectonic evolution of NW Mexico

Ricardo Vega-Granillo[1,*], Sergio Salgado-Souto[2], Saúl Herrera-Urbina[1], Víctor Valencia[3], and Jesús Roberto Vidal-Solano[1]

[1] Departamento de Geología, Universidad de Sonora. Rosales y Luis Encinas S/N, 83000 Hermosillo, Sonora, México.
[2] Department of Geosciences, The University of Arizona, 85721, Tucson, AZ, USA.
[3] Valencia Geoservices, 3389 N River Rapids Dr, 85712, Tucson AZ, USA.
** rvega@ciencias.uson.mx*

ABSTRACT

The Río Fuerte Formation, cropping out in Sinaloa state of northwestern Mexico, has been ascribed to the Middle to Late Ordovician based on its fossil content. U-Pb detrital zircon study in a rock sample of this unit yielded peaks at 521 Ma, 605 Ma and 881 Ma. Relative-age probability plots in the region suggest that the Río Fuerte Formation deposited in a basin located between Laurentia and an inactive peri-Gondwanan arc. Thermobarometric and petrographic studies of the Río Fuerte Formation indicate an initial low P/T or Buchan type metamorphic event. Structural analysis indicates that this event had a ~N-S shortening direction, and may be related to the collision of peri-Gondwanan blocks during the final amalgamation of Pangaea. In the same region, a granitic clast within an andesitic meta-agglomerate of the Topaco Formation yielded a 151 ± 1 Ma age, which predates a second tectono-metamorphic event. This event is ascribed to a Late Jurassic overprint in the El Fuerte region, which may be related to collision of an ophiolite block against the North American plate and is coeval with the Nevadan Orogeny of the North American Cordillera.

Key words: Buchan metamorphism, peri-Gondwanan, Nevadan, El Fuerte, Mexico.

RESUMEN

En el norte de Sinaloa, México, aflora la Formación Río Fuerte considerada de edad Ordovícico Medio a Tardío con base en sus fósiles. La determinación de edades U-Pb en circones detríticos en rocas de dicha unidad produjo un diagrama de probabilidad con picos a los 521, 605 y 881 Ma. Los diagramas de probabilidad de edades en esa unidad sugieren que la cuenca donde se depositó la Formación Río Fuerte se ubicaba en un océano entre Laurencia y Gondwana, cercano a un arco inactivo peri-Gondwaniano. Datos termabarométricos y estudios petrográficos de la Formación Río Fuerte indican la existencia de un primer evento de metamorfismo regional orogénico de baja P/T o de tipo Buchan. Estudios estructurales y relaciones geológicas indican que el evento tectono-metamórfico tuvo una dirección de acortamiento ~N-S y antecede al Jurásico Tardío. Con base en estos datos, interpretamos que dicho evento puede estar asociado a la colisión de bloques peri-Gondwanianos contra Laurencia durante la amalgamación final de Pangea. La edad de 151 ± 1 Ma obtenida en un clasto granítico contenido en un meta-aglomerado andesítico de la Formación Topaco, antecede a un evento de metamorfismo regional orogénico que afectó a dicha unidad. El segundo evento tectono-metamórfico, adscrito al Jurásico más tardío, afectó las rocas de la región de El Fuerte y pudo ser causado por la colisión de un bloque ofiolítico contra la placa Norteamericana. Este evento es contemporáneo con la orogenia Nevadiana de la Cordillera Norteamericana.

Palabras clave: metamorfismo Buchan, peri-Gondwaniano, Nevadiana, El Fuerte, México.

Vega-Granillo, R., Salgado-Souto, S., Herrera-Urbina, S., Valencia, V., Vidal-Solano, J.R., 2011, Metamorphism and deformation in the El Fuerte region: their role in the tectonic evolution of NW Mexico: Revista Mexicana de Ciencias Geológicas, v. 28, núm. 1, p. 10-23.

INTRODUCTION

At least three different regional metamorphic complexes compose the basement of terranes in northwestern Mexico (inset in Figure 1). These complexes are exposed in kilometer-scale tectonic windows excavated on younger sequences. In northeastern Sonora, the basement of the Chihuahua terrane (Campa and Coney, 1983) is the Mazatzal province (*e.g.*, Baldridge, 2004) consisting of Precambrian (~1.7 Ma) greenschist-amphibolite-facies volcanic and sedimentary rocks (Anderson, *et al*., 1980; Anderson and Silver, 1981; 2005). In northwestern Sonora, the basement of the Caborca terrane is regarded to be either part of the Yavapai or Mojave provinces consisting of Precambrian (~1.8-1.6 Ma) greenschist-amphibolite-facies plutonic, volcanic and sedimentary rocks (Anderson and Silver, 2005; Farmer *et al*., 2005). Basements of both, Caborca and Chihuahua terranes are intruded by ~1.4 and ~1.1 granites (Anderson *et al*., 1980; Shannon *et al*., 1997; Anderson and Morrison, 2005) and overlain by Neoproterozoic to Middle Permian platform successions (Stewart, 2005; Poole *et al*., 2005). A hypothetical Late Jurassic sinistral megashear was proposed to account for the speculative tectonic juxtaposition of the Caborca against the Chihuahua terrane (Anderson and Silver, 2005). However, both blocks are part of the Laurentian craton (*e.g.*, Baldridge, 2004). The third metamorphic complex crops out about 300 km farther south of the limits of the Laurentian craton. This complex is known as the Sonobari complex (de Cserna and Kent, 1961) or the Sonobari terrane (Campa and Coney, 1983). This terrane supposedly underlies the Jurassic to Lower Cretaceous Guerrero terrane (Figure 1) composed of volcanic, volcanosedimentary and minor sedimentary rocks (Campa and Coney, 1983). The Sonobari terrane includes metamorphosed volcanic and sedimentary rocks of the Río Fuerte Group, and the amphibolite-facies, plutonic, volcanic and sedimentary rocks of the Francisco Gneiss (Mullan, 1978; Keppie *et al*., 2006). Alternatively, these units were included by Sedlock *et al*. (1993) in their Tahué terrane, composed of middle Paleozoic metasedimentary rocks of unknown origin accreted to North America by Late Jurassic time. Finally, Poole *et al*. (2005) grouped the El Fuerte Group and Francisco Gneiss within the El Fuerte block, which also would include Upper Paleozoic rocks exposed in the San José de Gracia and San Javier areas (Sinaloa, Mexico). Vega-Granillo *et al*., (2008) based on geochronology of detrital zircons proposed an exotic origin for the Río Fuerte Formation with respect to the Laurentian craton.

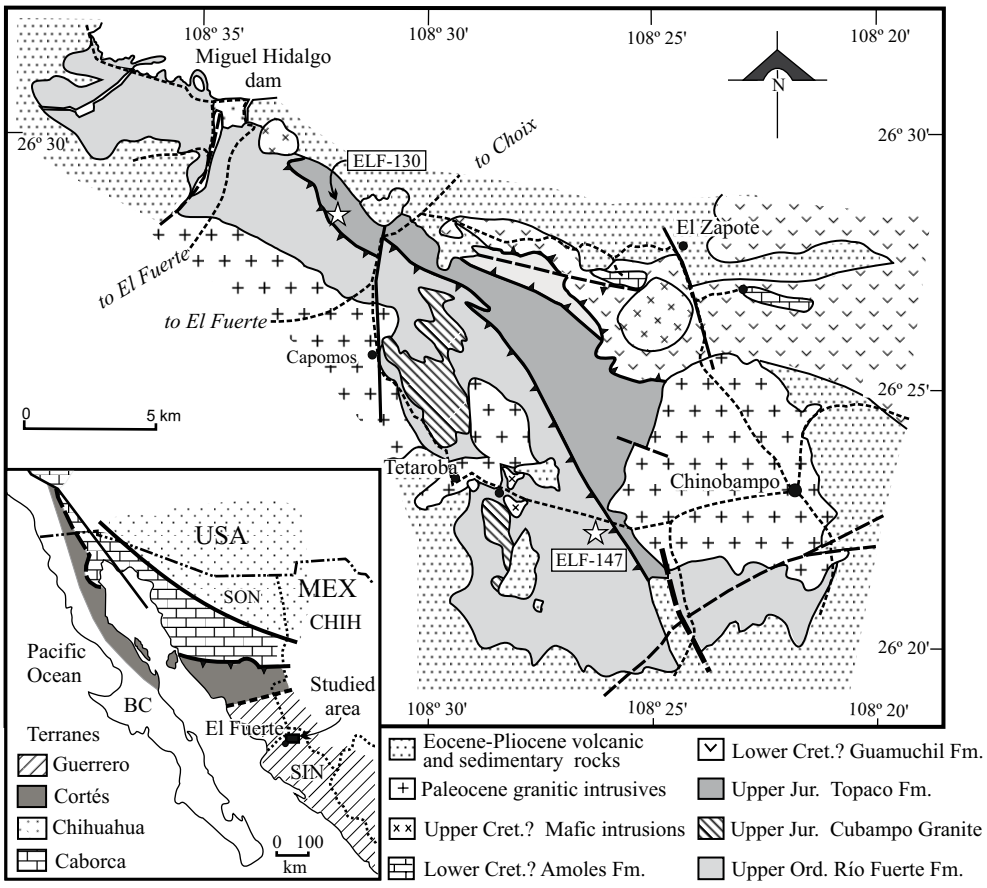

Figure 1. Geological map of the El Fuerte region (modified from Mullan, 1978). Inset shows the terrane subdivision (modified from Campa and Coney, 1983; and Poole *et al*., 2005). BC: Baja California; CHIH: Chihuahua; SIN: Sinaloa; SON: Sonora.

The Sonobari terrane is poorly known and its contacts, internal stratigraphy, structure, and tectonic setting remain undefined (Campa and Coney, 1983; Sedlock *et al*., 1993; Poole *et al*., 2005). The scarce understanding of the geology of this terrane can be attributed either to internal complexities related to overprinting of deformational and metamorphic events, and limited exposures. However, metamorphic rocks of the El Fuerte region are critical to understand the tectonic evolution of northwestern Mexico. Their location outboard of the Sonora-Marathon-Ouachita fold-and-thrust belt (Poole *et al*., 2005), suggests a different origin and metamorphic evolution from the Laurentian blocks of central and northern Sonora. This study is focused on defining the orogenic regional metamorphic events and correlated deformational phases of the Río Fuerte Group, a crucial element of the Sonobari terrane, through petrologic, structural, and microtectonic analyses. In addition, geochronologic studies were performed to supplement our interpretation of geologic events and to review the stratigraphy proposed by Mullan (1978). We also present the first thermobarometric study of the El Fuerte metamorphic rocks. Based on these data, we discuss the tectonic scenarios previously proposed for northwestern Mexico, and present a more comprehensive interpretation of the geologic evolution of this region.

GEOLOGICAL SETTING

In the El Fuerte region, Mullan (1978) recognized three metamorphic units: 1) metasedimentary and metavolcanic rocks of the Río Fuerte Group presumably of upper Paleozoic age; 2) amphibolite-facies rocks of the Francisco Gneiss; and 3) a thick sequence of Mesozoic, non-foliated, metavolcanic rocks of the El Zapote Group (Figure 1). The Río Fuerte Group, as formerly defined by Mullan (1978), included the Río Fuerte, Corral Falso and Topaco formations. The Río Fuerte and Corral Falso formations are metasedimentary successions composed of intercalated quartzite, schist and phyllite (Figure 2a). A thin marbleized limestone bed in the Río Fuerte Formation yielded Middle to Late Ordovician conodonts (Poole *et al*., 2005). These rocks display at least two main foliations, while another two are locally preserved. Superposed folding and sparse exposures prevent assigning a type section or thickness for the Río Fuerte or Corral Falso formations.

The Topaco Formation consists mostly of metamorphosed, dark-green agglomerate intercalated with minor meta-andesite and meta-rhyolite lava flows (Figures 2c-2d). Meta-agglomerates contain clasts of volcanic rocks, aplite, and metasedimentary rocks, the latter petrologically similar to those of the adjacent Río Fuerte Formation. In the northeastern area, the Río Fuerte Formation is thrusted over the Topaco Formation and foliations, in both units, trend to parallelism. Orogenic regional greenschist-facies metamorphism and micro- and mesoscopic-scale pervasive foliations in the Río Fuerte and Topaco formations were assigned to the Late Jurassic Nevadan Orogeny by Mullan (1978).

Mullan (1978) envisaged a conspicuous felsic rock, which he informally named the nodular rhyolite member, as a flow separating the Río Fuerte Formation from the overlying Corral Falso Formation, as well as the lower and upper members of the Topaco Formation (Figure 2b). Consequently, Mullan (1978) considered the metasedimentary Corral Falso Formation as a lateral variation of the metavolcanic lower member of the Topaco Formation. However, this felsic rock yielded a 155 ± 4 Ma age (U-Pb, zircon) (Vega-Granillo *et al*., 2008) indicating that is an aplite sill emplaced along the foliation of the metasedimentary rocks instead of a volcanic flow that could be used as a stratigraphic marker. Thus, discarding the felsic rock criteria as a marker layer, the Río Fuerte and the Corral Falso formations cannot be clearly separated, and they are regarded as a single unit named the Río Fuerte Formation (Vega-Granillo, *et al*., 2008). The Cubampo Granite intrudes the Río Fuerte Formation. This granite displays an incipient foliation and yielded a U-Pb zircon age of 151 ± 3 Ma (Vega-Granillo, *et al*., 2008). The nodular aplite and the Cubampo Granite are considered as part of the same intrusive suite based on similarities, both in petrology and age (Vega-Granillo *et al*., 2008). A summary of the stratigraphy is displayed in Figure 3.

The Francisco Gneiss (Mullan, 1978) is mainly composed by ortho- and paragneisses intercalated with tabular amphibolites. This unit is exposed in the south edge of the Sierra Sonobari, located west of the El Fuerte region. Mullan (1978) considered that the Francisco Gneiss may be the basement of the Río Fuerte Group, in spite of both units are exposed separately. Based on lithology and metamorphic imprint, Mullan (1978) tentatively correlated the Francisco Gneiss with Paleoproterozoic gneisses that crop out 300 km further north in Sonora. However, the Francisco Gneiss has yielded U-Pb zircon ages ca. 220-206 Ma (Late Triassic) (Anderson and Schmidt, 1983; Keppie *et al*., 2006, respectively), which are regarded as the protolith age. Consequently, these Upper Triassic rocks cannot be the basement of the Ordovician Río Fuerte Formation, nor can be correlated with Paleoproterozoic rocks of northern Sonora.

The El Zapote Group was regarded by Mullan (1978) as Early Cretaceous in age based on lithological correlation. This group includes the Guamúchil Formation consisting of a thick sequence of metabasites, which is overlain by the Los Amoles Formation consisting of ~100 m of nonfossiliferous limestones. The El Zapote Group overthrusts the Río Fuerte and Topaco Formations. Based on ages assigned by lithological correlation, Mullan (1978) considered that overthrusting occurred by Late Cretaceous-Paleogene times. The Río Fuerte and the Topaco formations, as well as the El Zapote Group are intruded and contact metamorphosed by the Capomos and Chinobampo granites (Mullan, 1978). The Capomos granite yielded a K-Ar on biotite age of 57.2 ± 1.2 Ma (Damon *et al*., 1983). Tertiary volcanic and

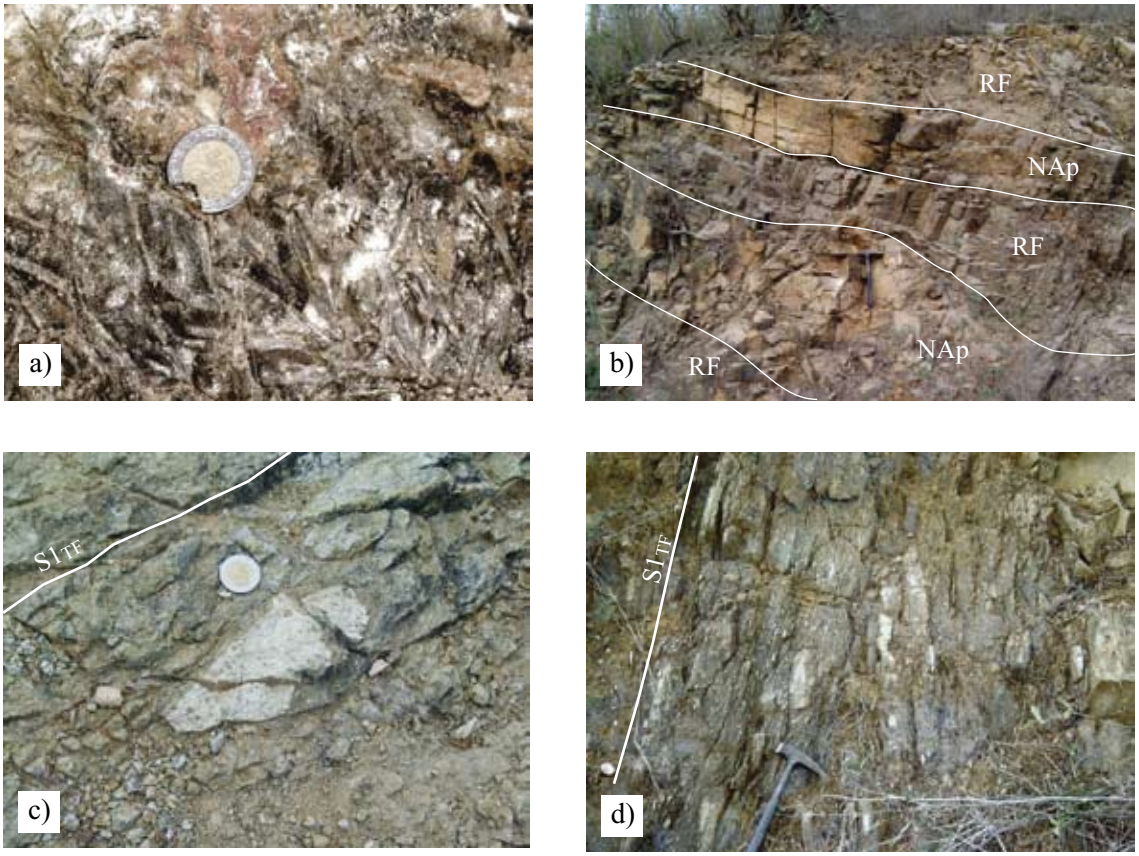

Figure 2. Exposures of the studied units from the El Fuerte region. a: Detail of andalusite mica schist of the Río Fuerte Formation (coin-diameter = 2.5 cm); b: Nodular aplite sill emplaced along the $S1_{RF}$ foliation of phyllite and quartzite of the Río Fuerte Formation (RF=Río Fuerte Fm; NAp=nodular aplite); c: Nodular aplite clast in meta-agglomerate of the Topaco Formation (dated in this paper); d: Meta-agglomerate in the Topaco Fm.

sedimentary rocks partially cover in angular unconformity the older rocks.

ANALYTICAL METHODS

U-Pb geochronology of zircons was carry out by laser ablation multicollector inductively coupled plasma mass spectrometry (LA-MC-ICPMS) at the Arizona LaserChron Center, following procedures of Gehrels *et al*. (2006) for detrital zircons, and Valencia *et al*. (2005) for magmatic zircons. Previously, the zircons were studied through cathodoluminiscence. For the igneous sample (ELF-130), the weighted mean of 25 individual analyses was calculated according to Ludwig (2003). The age error for the sample was calculated adding quadratically the two components (random or measurement error and systematic error). For the studied sample, error is ~0.79 % or ~1.2 Ma. All age uncertainties are reported at the 2σ level.

For provenance analysis, the detrital zircons are analyzed at random, with laser pits located in core portions of grains for consistency. In the ELF-147 sample, we analyzed 29 zircon grains to establish the main age groups. Data are filtered according to precision ($^{206}Pb/^{238}U$ and $^{206}Pb/^{207}Pb$ typically 5 % error cutoff) and discordance (typically 30% cutoff) and then plotted on Pb/U concordia diagrams and relative-age probability plots (using algorithms of Ludwig, 2003) or cumulative probability plots.

Mineral chemistry was performed using a CAMECA SX-50 electron microprobe at the Department of Lunar and Planetary Sciences, the University of Arizona. Analytical technique consisted of a beam current of 20.0 nA and an accelerating voltage of 15 kV. Counting time was 10 seconds for sodium and 20 seconds for other elements. Under these methods, contents below 0.1 % are considered out of the detection limits. Microprobe analytical error varies roughly between ± 0.01 to 0.04 wt % (1σ). In order to define the thermobarometric conditions, point chemical analyses were performed in the rim of selected adjoin minerals in two samples.

GEOCHRONOLOGY

Zircon concentrates were separated from two rock samples and dated by U-Pb geochronology in order to constrain the age of the Río Fuerte and Topaco Formations. Sample ELF-147 was collected at Los Mautos creek (UTM:

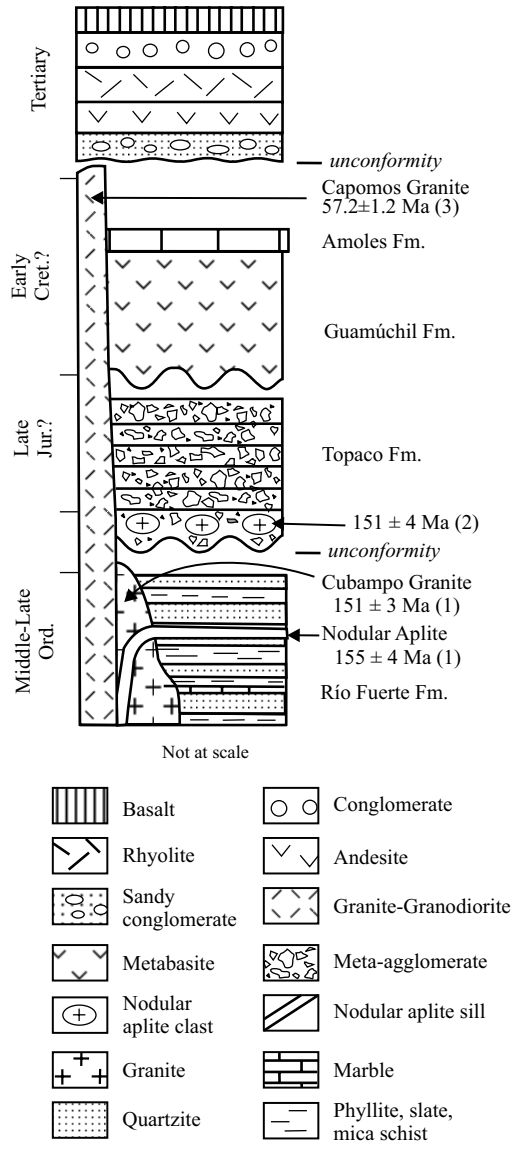

Figure 3. Schematic stratigraphy column of El Fuerte region. 1: U-Pb zircon ages from Vega-Granillo *et al*. (2008); 2: U-Pb zircon age, this paper; 3: K-Ar biotite age from Damon *et al*. (1983).

12-R, 0756049 W – 2919376 N) in a region formerly mapped as the lower member of the Topaco Formation (Mullan, 1978). This rock is a greenish chlorite-sericite-quartz phyllite derived from pelitic rock, which is intercalated with white-grey quartzites. The phyllite is a fine-grained rock composed of thin lenses of quartz, separated by thin sericite-chlorite-quartz cleavage domains. In a mesoscopic scale, this rock displays a complex fabric with at least three overprinting cleavages. Zircons of this sample have a reduced size range; generally they are prismatic, euhedral to subhedral, some have inherited zircons near of their centers and thin external zonation. As indicated in the analytical methods, zircons for provenance studies were randomly selected. In this sample, 27 detrital zircon ages define the main clusters (Figure 4b). Zircon ages cover a wide range: from 2,394 Ma to 466 Ma (Table 1). Only the 521 Ma, 605 Ma and 881 Ma peaks come from clusters of three or more zircons, and thus, they are considered statistically meaningful. Anyway, main peaks previously recognized in the Río Fuerte Formation (Vega-Granillo *et al*., 2008) are represented by ages obtained in the ELF-147 sample.

Sample ELF-130 was collected at UTM: 12R, 0745732 W – 2930610 N. This rock is a felsic igneous clast reworked in a greenish meta-agglomerate of the Topaco Formation, near the contact with the Río Fuerte Formation. In thin section, sample ELF-130 has elongate, spheroidal porphyroclasts of quartz and angular porphyroclasts of plagioclase in a very fine-grained matrix of quartz and feldspar. The cleavage is defined by preferred orientation of prismatic actinolite and elongation of quartz and plagioclase porphyroclasts. Cleavage of the clast is parallel to that of the enclosing meta-agglomerate. This felsic rock is petrologically similar to the nodular aplite. Zircons on this sample are prismatic, short, unzoned, and without inherited zircons. In this sample, 25 zircons (Table 2) yielded a mean age of 151 ± 1 Ma, and a mean square weighted deviation (MSWD) of 0.95 (Figure 4a).

METAMORPHISM AND THERMOBAROMETRY

Río Fuerte Formation

Metamorphic assemblages of the Río Fuerte Formation are summarized in the Table 3. These assemblages are dominated by muscovite + quartz + chlorite; or muscovite + quartz + biotite. Metamorphic grade gradually increases from northeast to southwest. In the lower to middle-grade zone, large fibrous pyrophyllite coexists with andalusite porphyroblasts. In the medium- and high-grade zones, andalusite porphyroblasts are common and generally larger than 0.5 cm, but locally they can reach 10 cm in length. Staurolite porphyroblasts (Figures 5a-5b) and fibrolitic sillimanite are found in limited areas of the higher-grade zone. Garnet is uncommon, as it was only found in one of the studied samples (Figure 5c). Grain-size is related to metamorphic grade; low-grade rocks are slates or phyllites, while high-grade rocks are schists with matrix made of ~1 mm grains.

Chemical analyses were performed in schist of the Río Fuerte Formation in order to define thermobarometric conditions. The sample ELF-10 (UTM 12R; 0740645 W – 29289940 N) is composed of muscovite, biotite, quartz, and garnet. Temperature was defined using the biotite-garnet (Bt-Grt) geothermometer of Battacharya *et al*. (1992) and the muscovite-garnet (Ms-Grt) geothermometer of Hynes and Forest (1988) (abbreviations in text and Table 3 are after Spear, 1995). Twelve Bt-Grt pairs yielded a temperature range of 480 ºC to 512 ºC, while seven Ms-Grt analyses yielded a temperature range between 477 ºC and 505 ºC. Pressure was estimated from the silicon content in

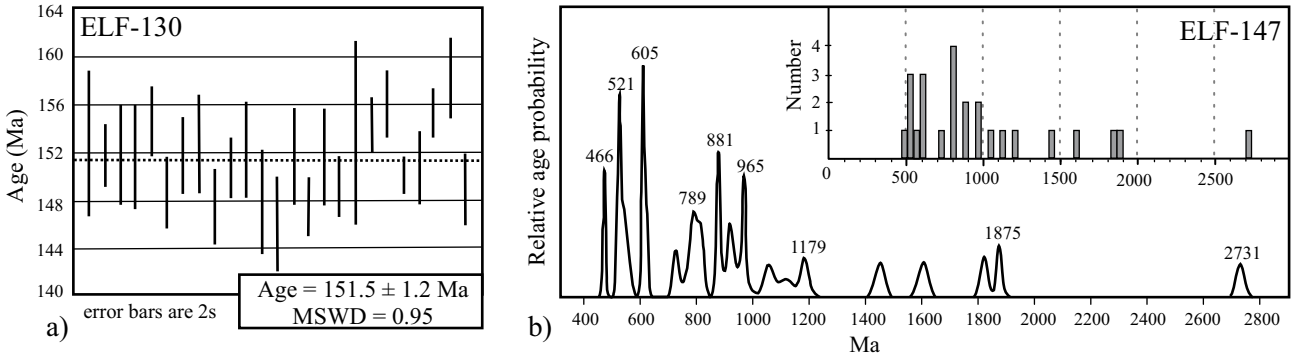

Figure 4. a: Weighted-average age of $^{206}Pb/^{238}U$ ages obtained for the nodular aplite (sample ELF-130) reworked in andesitic meta-agglomerate of the Topaco Formation; b: Relative-age probability plot of detrital zircon for phyllite of the Río Fuerte Formation (formerly lower member of the Topaco Formation).

muscovite, according to the Massonne and Schreyer (1987) calibration. Content of silicon atoms in the formula of 10 muscovite crystals varied from 3 to 3.13, indicating minimum pressures of 2 to 3 kbars, whereas a maximum pressure of ca. 4 kbar is suggested by the conspicuous presence of andalusite (Holdaway, 1971).

Mineral assemblages of metapelites from the Rio Fuerte Formation clearly define a transition from low-grade (greenschist facies) to medium-grade (amphibolite facies) metamorphism (Figure 6). Some mineral assemblages indicate key chemical reactions that have been determined in petrographic grids, for example: pyrophyllite-andalusite, andalusite-staurolite, andalusite-staurolite-sillimanite (*e.g.*, Spear, 1995). Mineral reactions and thermobarometric data displayed in Figure 6 indicate that the Río Fuerte Formation underwent a low P/T (andalusite-sillimanite) type of metamorphism, or Buchan type. According to Spear (1995) this type of metamorphism, implying high thermal gradient and low pressure, is common in island arcs, ocean ridges, and contact aureoles settings, where high-level intrusions produce high temperature at relatively low pressure.

Topaco Formation

Typical mineral assemblage in metavolcanic rocks of the Topaco Formation is: albite + actinolitic amphibole + epidote + biotite + chlorite + quartz. Each of these minerals can predominate in different rocks of the unit. This assemblage is characteristic of volcanic rocks metamorphosed under greenschist facies conditions (*e.g.*, Spear, 1995).

Chemical analyses were performed on a garnet amphibolite, sample ELF-157 (UTM 12R 29288549; 747231), originally regarded as part of the Topaco Formation (Salgado-Souto, 2006). This rock is a xenolith within dikes of the nodular aplite. Mineralogy of this xenolith is Mg-hastingsite + plagioclase An_{27-37} + garnet (Alm_{56-69}, Sps_{15-25}, Gro_{12-20}, And_{1-3}, Py_{1-3}) + epidote + quartz. The garnet-amphibole geothermometer (Graham and Powell, 1984) for this sample indicates a temperature range from 527 °C to 595 °C (Figure 6). The garnet-amphibole-plagioclase-quartz geothermobarometer of Kohn and Spear (1989) indicates a pressure range from 6.5 to 7.4 kbar and temperatures coincident with those obtained from the Graham and Powell (1984) geothermometer. Paragenesis and P-T conditions match those of epidote-amphibolite facies and correspond to Barrovian-type metamorphism (*e.g.*, Spear, 1995).

STRUCTURAL GEOLOGY

At least four foliations can be recognized in rocks of the Río Fuerte Formation. The first two foliations are pervasive while the last two occur locally in the hinge zone of folds affecting the less-competent lithologies as phyllites and slates. In the next paragraphs RF subscripts represent the Río Fuerte Formation and TF subscripts represent the Topaco Formation. First foliation $S1_{RF}$ is a continuous cleavage or schistosity defined by the preferred orientation of mica plates (chlorite, biotite and white mica). Phyllites and schists display a poikiloblastic texture where large staurolite and andalusite crystals contain aligned inclusions of quartz and opaque minerals forming an internal foliation ($Si=S1_{RF}$; Figures 5a-5b), which is oblique or orthogonal to the foliation outside the poikiloblasts. Geometric relationships between staurolite and andalusite poikiloblasts with respect to the internal and external foliations, indicate that their growth is post-tectonic or syntectonic with respect to D1 (Figures 5a-5b). Then the metamorphic assemblage formed in the last stages of the D1 deformation is quartz + muscovite + biotite + andalusite + staurolite + sillimanite, because all those minerals are aligned along the $S1_{RF}$ foliation.

Second foliation $S2_{RF}$ is oblique or orthogonal with respect to the $S1_{RF}$ foliation. The $S2_{RF}$ foliation is penetrative at the microscopic scale, and locally transposes the structures formed during the first deformation phase. In thin section, relicts of the $S1_{RF}$ appear as intrafolial folds between the $S2_{RF}$ foliation planes. Mica and quartz recrystallization occurs along the $S2_{RF}$ foliation. Although internal foliation ($Si=S1_{RF}$) in andalusite is locally orthogonal or oblique to

Table 1. Geochronological data for sample ELF-147.

Analysis	U (ppm)	U/Th	Isotopic ratios					error corr.	Apparent ages (Ma)						Best age (Ma)	± (Ma)
			$^{206}Pb/^{204}Pb$	$^{207}Pb^*/^{235}U$	± (%)	$^{206}Pb^*/^{238}U$	± (%)		$^{206}Pb^*/^{238}U$	± (Ma)	$^{207}Pb^*/^{235}U$	± (Ma)	$^{206}Pb^*/^{207}Pb^*$	± (Ma)		
ELF147-1	742	3.0	64299	5.28585	1.4	0.33446	1.0	0.71	1860.0	16.2	1866.6	12.1	1873.9	18.0	1873.9	18.0
ELF147-2	914	1.5	18543	1.42515	1.8	0.14558	1.4	0.81	876.2	11.8	899.5	10.6	957.4	21.4	876.2	11.8
ELF147-3	372	3.3	9901	0.99436	4.2	0.11850	3.0	0.72	721.9	20.7	700.9	21.2	634.3	62.2	721.9	20.7
ELF147-4	2114	6.7	51436	1.25063	3.0	0.12985	2.8	0.94	787.0	20.7	823.7	16.8	924.1	20.6	787.0	20.7
ELF147-5	1573	3.1	13542	1.70327	3.3	0.16108	1.7	0.52	962.8	15.6	1009.8	21.4	1113.1	57.0	1113.1	57.0
ELF147-6	1357	2.2	64296	4.37680	7.6	0.28506	7.4	0.99	1616.8	106.5	1708.0	62.5	1821.6	23.4	1821.6	23.4
ELF147-7	1086	4.0	28918	1.50539	5.0	0.15352	4.8	0.96	920.7	41.5	932.6	30.8	960.8	28.9	920.7	41.5
ELF147-8	558	0.8	10181	0.82808	2.7	0.09880	2.2	0.83	607.3	12.8	612.5	12.3	631.8	32.5	607.3	12.8
ELF147-9	676	2.0	13003	0.58353	1.8	0.07501	1.5	0.82	466.3	6.6	466.7	6.7	469.0	22.9	466.3	6.6
ELF147-10	492	1.9	11184	0.67864	1.8	0.08443	1.3	0.76	522.5	6.8	526.0	7.3	540.9	25.4	522.5	6.8
ELF147-11	427	3.2	12674	1.21674	6.1	0.12945	5.3	0.86	784.7	38.9	808.3	34.0	873.7	63.8	784.7	38.9
ELF147-12	456	2.6	16029	1.61263	1.6	0.16149	1.0	0.62	965.0	9.0	975.1	10.2	997.9	26.0	965.0	9.0
ELF147-13	69	2.2	653	1.90963	17.2	0.15317	2.3	0.13	918.7	19.7	1084.5	115.3	1434.4	328.1	1434.4	328.1
ELF147-14	182	2.4	11788	2.23812	1.6	0.20457	1.0	0.61	1199.8	10.9	1193.1	11.6	1180.8	25.9	1180.8	25.9
ELF147-15	650	2.5	6418	0.70133	3.0	0.08368	2.3	0.77	518.0	11.4	539.6	12.4	631.7	41.1	518.0	11.4
ELF147-16	469	0.8	10191	0.83114	1.4	0.09847	1.0	0.69	605.5	5.8	614.2	6.7	646.8	22.5	605.5	5.8
ELF147-17	718	2.3	23853	1.61037	6.2	0.15936	6.1	0.99	953.2	54.0	974.3	38.7	1022.0	20.3	953.2	54.0
ELF147-18	509	4.5	9887	0.84524	1.5	0.10030	1.1	0.72	616.2	6.3	622.0	6.9	643.3	22.1	616.2	6.3
ELF147-19	313	3.0	7147	1.53803	3.0	0.15210	2.2	0.75	912.7	19.0	945.7	18.4	1023.3	40.2	912.7	19.0
ELF147-20	542	1.9	4257	11.72367	4.8	0.44973	4.5	0.93	2394.1	89.2	2582.6	44.9	2734.0	29.0	2734.0	29.0
ELF147-21	718	2.3	9274	3.15435	4.2	0.23127	3.9	0.93	1341.1	47.0	1446.1	32.2	1603.9	28.8	1603.9	28.8
ELF147-22	228	3.0	11607	1.36938	1.9	0.14536	1.4	0.77	874.9	11.9	875.9	11.0	878.4	24.9	874.9	11.9
ELF147-23	2663	7.7	29169	0.79119	4.3	0.08926	4.0	0.94	551.2	21.2	591.8	19.1	751.1	29.9	551.2	21.2
ELF147-24	736	4.1	33489	1.75445	1.9	0.17101	1.0	0.54	1017.7	9.4	1028.8	12.0	1052.5	31.6	1052.5	31.6
ELF147-25	854	4.5	33460	1.28476	7.4	0.12912	7.2	0.98	782.9	53.3	839.0	42.2	990.5	30.8	782.9	53.3
ELF147-26	428	2.2	9799	0.70374	2.6	0.08653	2.4	0.92	535.0	12.4	541.0	11.1	566.5	23.0	535.0	12.4
ELF147-27	211	2.7	12063	1.31056	2.6	0.13425	2.4	0.92	812.1	18.2	850.4	14.9	951.6	20.7	812.1	18.2

Table 2. Geochronological data for sample ELF-130.

Analysis	U (ppm)	U/Th	Isotopic ratios					error corr.	Apparent ages (Ma)						Best age (Ma)	± (Ma)
			$^{206}Pb/^{204}Pb$	$^{207}Pb^*/^{235}U$	± (%)	$^{206}Pb^*/^{238}U$	± (%)		$^{206}Pb^*/^{238}U$	± (Ma)	$^{207}Pb^*/^{235}U$	± (Ma)	$^{206}Pb^*/^{207}Pb^*$	± (Ma)		
ELF130- 1	190	1.6	1359	0.17844	6.9	0.02399	4.1	0.60	152.8	6.2	166.7	10.6	369.0	124.8	152.8	6.2
ELF130- 2	214	2.3	4535	0.14769	7.3	0.02382	1.8	0.25	151.8	2.7	139.9	9.5	-57.7	172.1	151.8	2.7
ELF130- 3	182	2.3	1945	0.17370	7.5	0.02384	2.8	0.38	151.9	4.3	162.6	11.3	322.2	159.0	151.9	4.3
ELF130- 4	212	2.1	4951	0.15322	7.0	0.02379	2.9	0.41	151.6	4.3	144.8	9.5	34.1	154.1	151.6	4.3
ELF130- 5	209	2.2	3140	0.14501	5.7	0.02427	2.1	0.37	154.6	3.2	137.5	7.4	-148.0	132.6	154.6	3.2
ELF130- 6	191	2.0	3950	0.16313	6.9	0.02331	2.0	0.28	148.6	2.9	153.4	9.9	229.7	154.0	148.6	2.9
ELF130- 7	173	1.9	2952	0.16239	7.1	0.02381	2.2	0.31	151.7	3.3	152.8	10.1	170.0	158.8	151.7	3.3
ELF130- 8	1786	1.3	19781	0.16281	3.0	0.02398	2.8	0.92	152.8	4.2	153.2	4.3	159.1	28.0	152.8	4.2
ELF130- 9	218	2.1	3947	0.14892	9.3	0.02314	2.2	0.24	147.5	3.3	141.0	12.2	32.6	215.9	147.5	3.3
ELF130- 10	297	1.7	3742	0.16296	3.5	0.02367	1.7	0.51	150.8	2.6	153.3	4.9	192.2	69.4	150.8	2.6
ELF130- 11	253	1.9	4864	0.16028	4.4	0.02391	2.8	0.62	152.3	4.1	150.9	6.2	129.0	81.1	152.3	4.1
ELF130- 12	287	1.4	3766	0.15814	4.2	0.02321	3.0	0.73	147.9	4.4	149.1	5.8	167.9	66.9	147.9	4.4
ELF130- 13	203	1.5	3259	0.14559	7.7	0.02292	2.8	0.36	146.1	4.0	138.0	10.0	1.2	174.2	146.1	4.0
ELF130- 14	231	1.8	2979	0.15861	7.6	0.02382	2.7	0.36	151.7	4.1	149.5	10.6	113.8	168.7	151.7	4.1
ELF130- 15	184	2.1	2053	0.17053	5.9	0.02314	1.7	0.29	147.5	2.5	159.9	8.7	347.4	127.6	147.5	2.5
ELF130- 16	215	1.8	2919	0.14272	6.5	0.02381	2.7	0.42	151.7	4.1	135.5	8.2	-140.9	146.4	151.7	4.1
ELF130- 17	173	2.1	1528	0.16793	7.8	0.02340	1.8	0.23	149.1	2.7	157.6	11.3	287.5	172.6	149.1	2.7
ELF130- 18	261	2.4	14192	0.13999	11.1	0.02412	5.1	0.46	153.6	7.7	133.0	13.8	-220.6	248.1	153.6	7.7
ELF130- 19	454	1.5	2968	0.16370	3.0	0.02424	1.5	0.49	154.4	2.3	153.9	4.3	147.3	62.1	154.4	2.3
ELF130- 20	194	2.3	1418	0.16796	8.3	0.02451	1.8	0.22	156.1	2.8	157.7	12.1	181.2	188.2	156.1	2.8
ELF130- 21	414	1.1	6136	0.15497	2.5	0.02358	1.2	0.48	150.2	1.8	146.3	3.4	82.9	51.7	150.2	1.8
ELF130- 22	183	2.5	4203	0.15258	7.1	0.02367	2.1	0.29	150.8	3.1	144.2	9.5	36.8	162.2	150.8	3.1
ELF130- 23	437	1.8	4459	0.17907	2.5	0.02437	1.4	0.57	155.2	2.2	167.3	3.8	341.1	46.2	155.2	2.2
ELF130- 24	214	2.2	5734	0.17431	8.1	0.02484	2.2	0.27	158.2	3.4	163.2	12.2	235.9	180.3	158.2	3.4
ELF130- 25	188	2.4	3330	0.15336	8.0	0.02337	2.1	0.26	148.9	3.1	144.9	10.8	78.6	183.6	148.9	3.1

Table 3. Representative paragenesis in the Río Fuerte Formation.

Metamorphic grade	Paragenesis	Facies
Lower grade	Ms + Chl + Qtz Ms + Chl + Qtz + Prl	Greenschist facies
Low grade	Ms + Bt + Chl + Qtz Ms + Qtz + Prl + And Bt + Pl + Qtz Bt + Ms + And + Pl + Qtz	
Medium grade	Bt + Ms + Pl + Grt + Qtz Bt + And + St + Pl + Qtz Bt + St + Pl + Qtz	Amphibolite facies
Higher grade	Bt + St + Sill + Pl + Qtz	

Ms=Muscovite, Chl=Chlorite, Qtz=Quartz, Prl=Phyrophyllite, Bt=Biotite, Pl=Plagioclase, And=Andalusite, St=Staurolite, Sil=Sillimanite, Grt=Garnet.

$S2_{RF}$, parallelism between internal and external foliations suggests that andalusite poikiloblasts also crystallized during the second deformation event. The $D2_{RF}$ deformation-metamorphism event also can be recognized in some exposures, where mesoscopic isoclinal folds bending the $S1_{RF}$ foliation are trapped between the $S2_{RF}$ foliation.

The third $S3_{RF}$ and fourth $S4_{RF}$ foliations are spaced cleavages (Figures 7a, 7b, 7c) formed by mica-rich cleavage domains, which separate zones with random oriented crystals, known as microlithons. The third foliation has millimeter wide separations between cleavage domains, while the fourth cleavage has centimeter separation between cleavage domains. There is no mineral growth related to $S3_{RF}$ or $S4_{RF}$ foliations; only cleavage planes rich in opaque and/or micaceous material, which were left behind or concentrated by pressure-solution mechanism (*e.g.*, Passchier

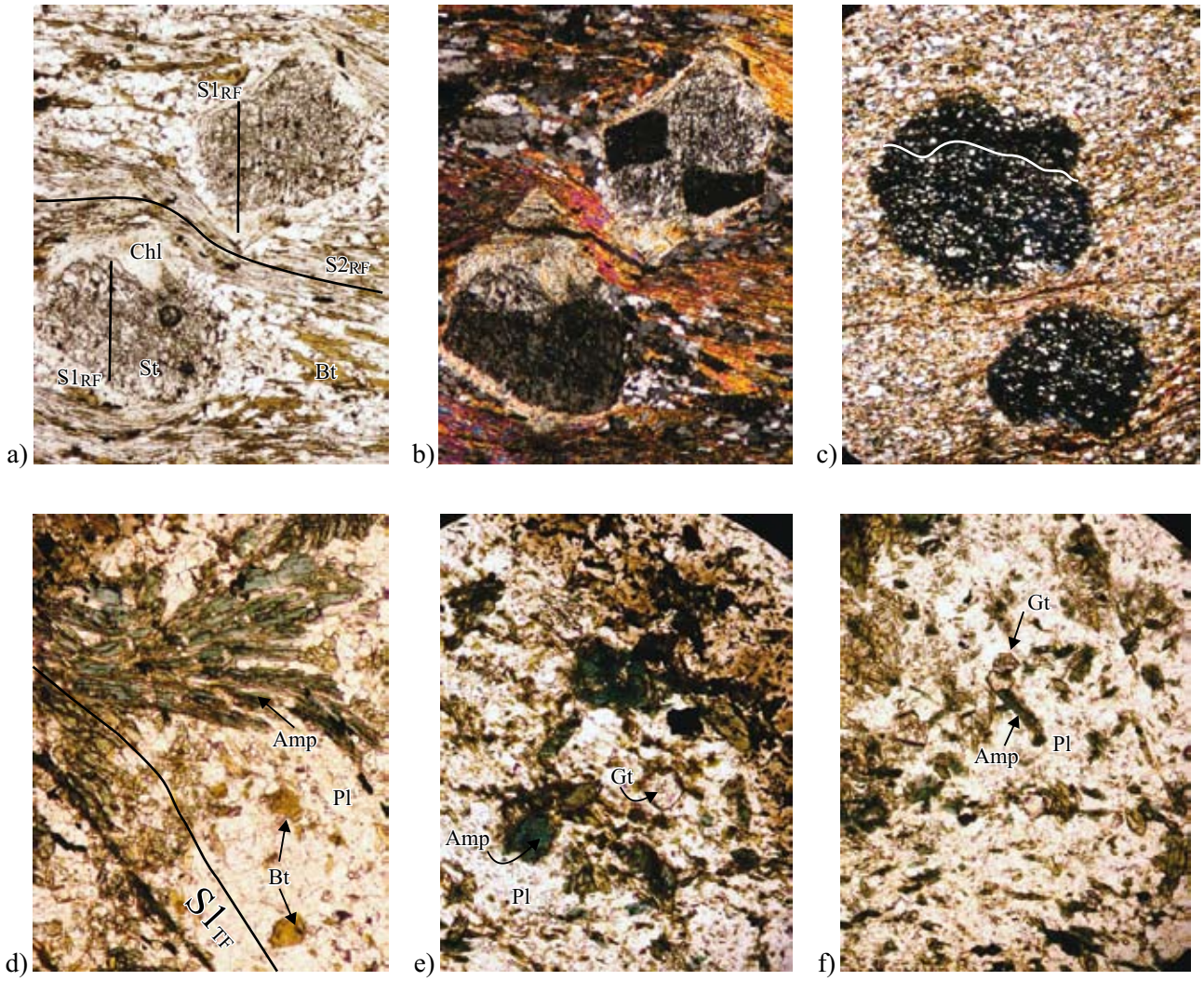

Figure 5. Selected photomicrographs of different lithotypes exposed in the El Fuerte region. a: staurolite mica schist of the Río Fuerte Formation; staurolite porphyroblasts (St) contain inclusions defining an internal ($S1_{RF}$) foliation perpendicular to the external ($S2_{RF}$) foliation; b: same picture but with crossed nicols; an hourglass twin can be seen in one of the staurolite crystals; c: garnet phyllite of the Río Fuerte Formation; only one foliation is visible, which is continuous within the garnet porphyroblasts (black); d: amphibolite from the Topaco Fm; large fibro-radial amphibole crystals in microlithons between the spaced cleavage ($S1_{TF}$); e and f: garnet amphibolite xenolith within a nodular aplite dike (Amp=amphibole; Gt=garnet; Pl=plagioclase).

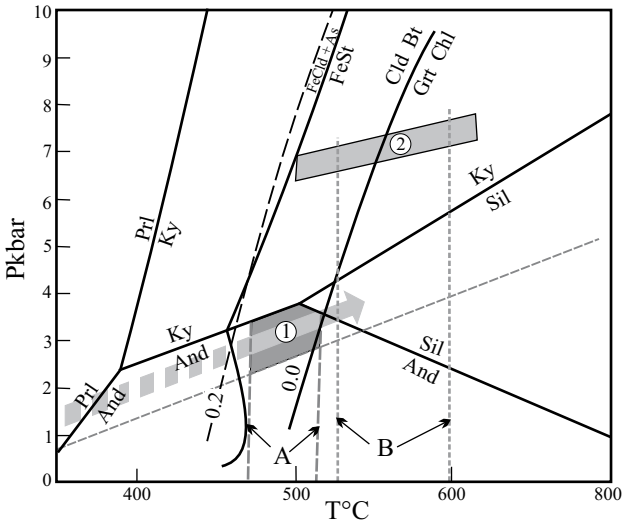

Figure 6. P-T diagram showing the estimated metamorphic conditions for the Río Fuerte and Topaco formations. 1) Conditions of the sample ELF-10 collected from the Río Fuerte Formation; 2) conditions of the sample ELF-157, a metabasite xenolith within a nodular aplite dike. A) Temperature range defined with Bt-Grt and Ms-Grt geothermometers; B) temperature range defined with the Grt-Amp geothermometer. Discontinuous grey arrow indicates trends of paragenesis displayed by Río Fuerte rocks. Lines with numbers (0.2, 0.0) indicate the Mn content in garnet for the reaction: Cld + Bt = Grt + Chl (see Spear, 1995). Cld is for chloritoid; other abbreviations as in Table 3.

and Trouw, 1996). The third and fourth cleavages are developed locally in the hinge zones of closed to thigh folds imposed on slates, phyllites, and mica schists, but do not transect the quartzite layers.

Meta-agglomerates of the Topaco Formation display a pervasive foliation $S1_{TF}$ (Figures 2c, 2d) produced by preferred orientation of amphibole and mica crystals. Igneous and metamorphic clasts are elongated parallel to this foliation. In thin section, the main fabric is a spaced foliation ($S1_{TF}$) with cleavage domains composed of fine-grained amphibole, chlorite, and biotite that separates microlithons of quartz + plagioclase, displaying a seriate-interlobate fabric. Larger amphibole crystals in microlithons retain a random fabric (Figure 5d) indicating a pre-tectonic crystallization of these minerals. The rocks of the Topaco Formation display a second foliation $S2_{TF}$. This cleavage occurs locally in the hinges of closed folds, where is oblique with respect to $S1_{TF}$. This cleavage is evidenced by dark seams of chlorite and opaque minerals, without mineral growth along the foliation planes. This suggests that the younger cleavage was formed by pressure-solution mechanism (*e.g.*, Passchier and Trouw, 1996).

Foliation structural data are illustrated in Figure 8. Figures 8a-8b represents the first foliation $S1_{RF}$ in the Río

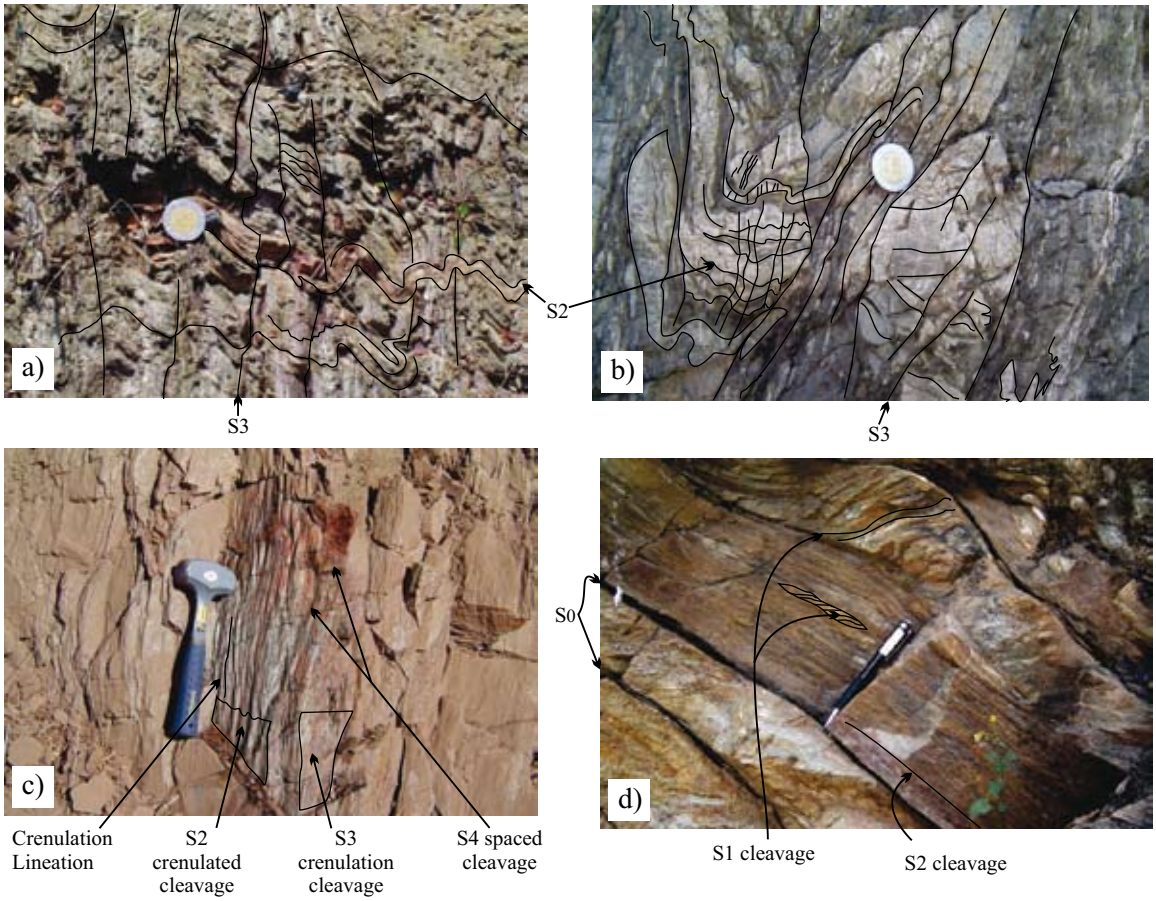

Figure 7. Outcrop photographs of main foliations in the Río Fuerte Formation. a: Mica schist with crenulation cleavage; b: boudinaged quartzite layers intercalated with black slate; c: muscovite-chlorite phyllite; d: quartzite and phyllitic quartzite.

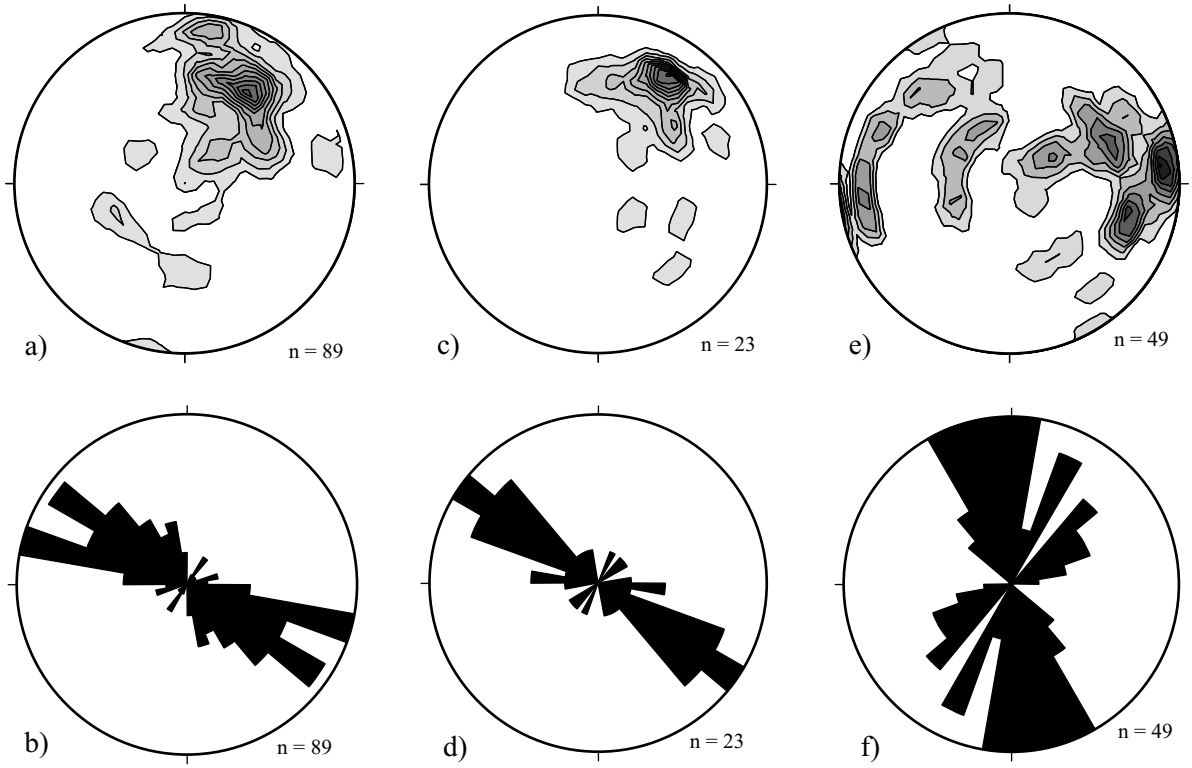

Figure 8. a: Density contour diagrams from poles of the first foliation in the Río Fuerte Formation, and c: Topaco Formation; e: density contour diagram from poles of the younger foliations in the Río Fuerte and Topaco units respectively. b and d; rose diagrams of foliation strikes in the Rio Fuerte and Topaco formations respectively; f: rose diagram of S3 and S4 foliation strikes in the Río Fuerte and Topaco formations. In a, c and e, equal area, lower hemisphere projection was used.

Fuerte Formation and Figures 8c-8d represents the first foliation $S1_{TF}$ in the Topaco Formation. There is a close correspondence between both diagrams, with main strike directions between N50°- 60°W and main dip directions between 30°- 40°SW. This indicates a trend to parallelism between the foliations in those units. However, the Río Fuerte plot displays a cluster of foliation data with strikes mainly between N70°- 80°W and dips mostly between 10°-20°SW, which is not present in the Topaco Formation. The Figures 8e-8f represents the S3 and S4 foliations related to the D3 and D4 deformation phases. These foliations have two main attitudes: S3 is characterized by strikes between N30°W and N10°E and dips between 60°SW and 80°NW, whereas S4 is characterized by strikes between N20°-50°E and dips between S40°-70°E.

DISCUSSION

Stratigraphic and paleogeographic implications

The 151 ± 1 Ma age of the granitic clast (sample ELF-130) reworked into meta-agglomerate of the Topaco Formation is equal to the 151 ± 3 Ma age of the Cubampo Granite and is equivalent within error with the 155 ± 4 Ma age reported for a sill of the nodular aplite (Vega-Granillo *et al.*, 2008). Also, the composition and fabric of the clast match those of the nodular aplite sill. Therefore, deposition of the upper member of the Topaco Formation followed the intrusion and exhumation of the Late Jurassic Cubampo Granite and nodular aplite sills. Although the minimum age is unconstrained, the Topaco Formation is regarded as latest Jurassic in age because it is overlain by the El Zapote Group composed of volcanic rocks and limestone considered to be Early Cretaceous in age (Mullan, 1978). Meta-agglomerate also contain clasts of phyllite, schists and quartzites, which have petrologic and metamorphic characteristics similar to those of the Río Fuerte Formation. Clasts of aplite and metamorphic rocks reworked into the meta-agglomerates imply that the Topaco Formation was deposited on or adjacent to the Río Fuerte Formation. Both formations were originally separated by a major unconformity (Figure 3).

Relative-age probability plot for sample ELF-147 (Figure 4b), which is based on limited data, can be correlated with data obtained from the Río Fuerte Formation (Vega-Granillo *et al*., 2008). Although, the ELF-147 sample was obtained from a region originally mapped as the lower member of the Topaco Formation (Mullan, 1978), we consider that this region is part of the Río Fuerte Formation, based on petrological similarity, like the intercalations of quartzites and phyllites, and the lacking of any Jurassic or younger zircons in the studied sample. Then, we retain the Topaco Formation name only for the upper member of that unit. Also, we suggest that the Río Fuerte Group name,

proposed by Mullan (1978) to encompass the Río Fuerte and Topaco formations in a single unit, is artificial because these units were formed at very different times, are lithologically contrasting, and display different metamorphic histories.

Detrital-zircon plot reported here, in conjunction with those reported by Vega-Granillo *et al.* (2008) indicate that sediments of the Río Fuerte basin were supplied by Middle to Late Ordovician, Neoproterozoic-Early Cambrian (peri-Gondwanan), Mesoproterozoic (Grenvillian), and Paleoproterozoic to Archean sources (Figure 4). Detrital-zircon plots differ of those arising from the lower Paleozoic Laurentian successions of Sonora (Gehrels *et al.*, 1995; Gross *et al.*, 2000, Stewart *et al.*, 2001) and from the lower Paleozoic Gondwanan successions of the Oaxaca terrane (Gillis *et al.*, 2005). They also differ from the allochthonous Paleozoic terranes of Nevada, such as the Golconda and Roberts Mountains (Gehrels *et al*., 2000, Riley *et al*., 2000; Barbeau *et al*., 2005, and references therein), which have Laurentian affinity. However, detrital-zircon populations of sample ELF-147 are similar to those reported for the Ixcamilpa suite of the Mixteco terrane in southern Mexico (Talavera-Mendoza *et al*., 2005), which is interpreted to be a crustal fragment trapped between Laurentia and Gondwana during the Pangaea assembly (Talavera-Mendoza, *et al.*, 2005; Vega-Granillo *et al.,* 2007; 2009). Figure 9 shows relative-age probability plots from all the mentioned localities.

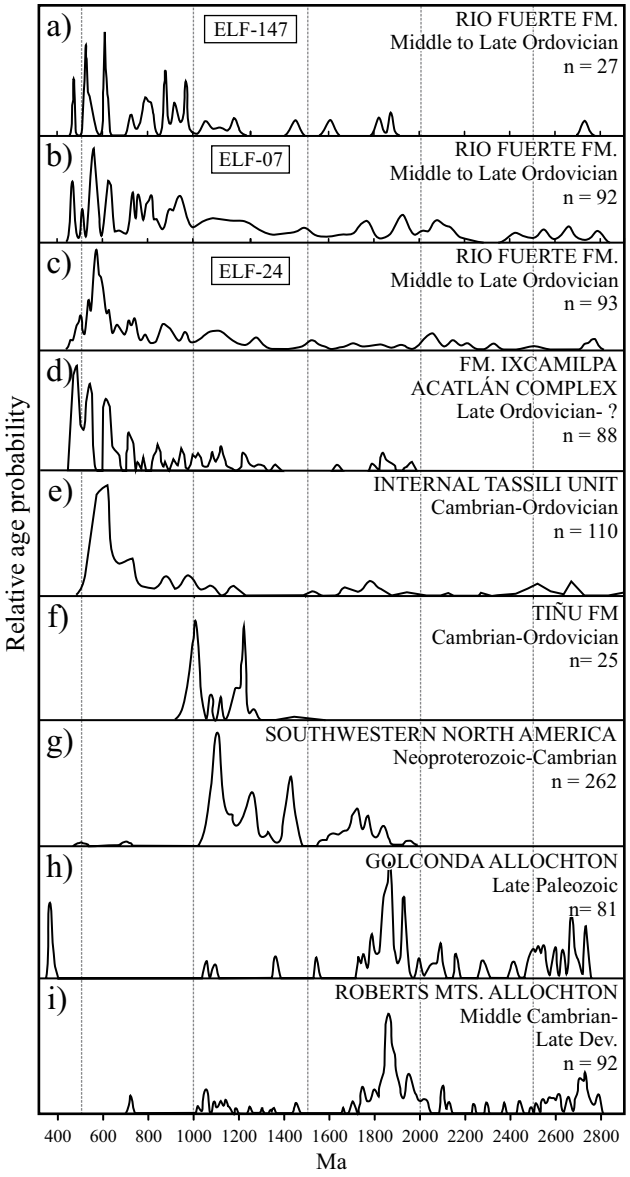

Figure 9. Relative age probability plots for rocks of selected areas. a: Río Fuerte Formation, this paper; b and c: Río Fuerte Formation, Sinaloa, Mexico (Vega-Granillo *et al*., 2008); d: Ixcamilpa Formation of the Acatlán Complex, Guerrero, Mexico (Talavera-Mendoza *et al*., 2005); e: Internal Tassili Unit of northern Gondwana, Africa (Avigad, *et al*., 2003); f: Tiñú Formation overlying the Oaxaca Complex, Oaxaca, Mexico (Gillis *et al*., 2005); g: southwestern North America (Gross *et al*., 2000; Stewart *et al*., 2001); h: Golconda Allochthon, Nevada, USA (Riley *et al*., 2000); i: Roberts Mountains Allochthon, Nevada, USA (Gehrels *et al*., 2000).

Tectonic evolution

Rocks of the Río Fuerte Formation exposed in the study area display four distinct superposed foliations, which are interpreted as the result of three different deformation events. The first deformation phase D1 produced the $S1_{RF}$ foliation. A metamorphic event ($M1_{RF}$) occurred before, during, and after the D1 event, producing a high-grade metamorphic assemblage. Lithology and low P/T character (andalusite-sillimanite series) of this event suggest a magmatic-arc tectonic setting, although further studies are required to confirm this hypothesis. Thermobarometry of a garnet-amphibolite xenolith indicates maximum pressure of ~7 kbar (~20 km depth), about 3 kbar higher than the estimated for the Río Fuerte metasediments. Also, the exposed rocks of the Topaco Formation lack of garnet. Accordingly, we consider that the garnet amphibolite is not part of the Topaco Formation but may correspond to a fragment of a unit underlying the Río Fuerte Formation, which was upraised by the aplitic magma.

Available structural data suggest a ~NNE-SSW shortening direction for the D1 event (Figure 8a). The first orogenic event should occur before the emplacement of the ca. 151 Ma aplitic sill along the $S1_{RF}$ foliation. However, there are no precise geochronological data to constrain the maximum age of the D1-M1 tectonic-metamorphic event. The ~NNE-SSW shortening direction that we deduced for the D1 phase coincides with that proposed by Poole and Madrid (1988) for a compressive phase causing the Carboniferous to Late Permian thrust of Paleozoic slope and abyssal successions over coeval platform successions in central Sonora. On this basis, we hypothesize that the first orogenic event imprinted in the Río Fuerte Formation may be related with the event proposed by Poole and Madrid (1988) in central Sonora. In a regional context, this first event may be related to the Laurentia-Gondwana final amalgamation, during which, the El Fuerte exotic block might have collided with

the southwestern margin of Laurentia. Given that higher-grade rocks in the Río Fuerte Formation occur preferentially along the western margin of the belt, where metamorphic rocks are intruded by the Capomos granite, Mullan (1978) regarded them as resulting from contact metamorphism. However, the Late Jurassic Cubampo Granite and nodular aplite transect and follow the first foliation of the Río Fuerte rocks indicating that metamorphism preceded that age, and consequently, also preceded the emplacement of the Paleocene Capomos Granite.

The second orogenic event in the El Fuerte region probably occurred in the latest Jurassic to earliest Cretaceous time, when a magmatic event is recorded by the intrusion of the Cubampo Granite and related nodular aplite sills. Afterward, the region was upraised and exhumed, and covered by volcanic rocks of the Topaco Formation. This is indicated by reworked metamorphic-rock and nodular aplite clasts in Topaco agglomerates. Subsequently, a major compressive event caused thrusting of the Río Fuerte unit over the Topaco unit, originating a second foliation ($S2_{RF}$) in the Río Fuerte Formation and a first foliation ($S1_{TF}$) in the Topaco Formation. As indicated by the structural data, the first foliation of the Río Fuerte Formation trends toward parallelism with the first foliation in the Topaco Formation ($S1_{TF}$). Structural data of the Topaco Formation (Figure 8c) indicate the D2 phase has a N30°-50°E shortening direction. This tectonic event is predated by the 151-155 Ma ages of the Cubampo Granite and nodular aplite, and postdated by volcanism of the El Zapote Group that was assigned to the Early Cretaceous by Mullan (1978). Consequently, the second event is coeval with the Nevadan orogeny in the western North American Cordillera (*e.g.*, Burchfiel *et al.*, 1992). In California, the Nevadan Orogeny involved underthrusting of island-arc rocks on the west and significant crustal shortening in the central and eastern belts (Schweickert *et al.*, 1984). The triggering force producing this regional tectonic shortening in northern Sinaloa is still poorly understood. In the Vizcaíno peninsula, western Baja California Sur, a Late Jurassic-earliest Cretaceous shortening event may be related to accretion of an ophiolite to North America (*e.g.*, Sedlock, 2003).

The third and fourth deformational phases produced closed to tight folding of the Topaco S1 foliation and superposed folding in the Río Fuerte Formation, as well as local axial planar cleavages ($S3\text{-}S4_{RF}$; $S2\text{-}S3_{TF}$) in the hinges of these folds. Available structural data indicate ~E-W shortening direction for the third phase, and ~WNW-ESE shortening direction for the fourth phase (Figure 8e). These deformations may be related to thrusting of the thick Cretaceous volcanic rocks of the El Zapote Group over the Topaco and Río Fuerte units. This thrusting might have occurred after the Early Cretaceous (?) deposition of the El Zapote Group and before the intrusion of Paleocene granites. Consequently, the third and fourth deformational phases probably occurred during a Late Cretaceous-Paleocene event.

ACKNOWLEDGMENTS

The research for this paper was financed by a CONACYT (79759) grant to Ricardo Vega-Granillo. We appreciate carefully comments by Dr. Forrest Poole and an anonymous reviewer.

REFERENCES

Anderson, J.L., Morrison, J., 2005, Ilmenite, magnetite, and peraluminous Mesoproterozoic anorogenic granites of Laurentia and Baltica: Lithos, 80(1-4), 45-60.

Anderson, T.H., Schmidt, V.A., 1983, A model of the evolution of Middle America and the Gulf of Mexico-Caribbean Sea region during Mesozoic time: Geological Society of America Bulletin, 94(8), 941-966.

Anderson, T.H., Silver, L.T., 1981, An overview of Precambrian rocks in Sonora: Revista, Universidad Nacional Autónoma de México, Instituto de Geología, 5(2), 131-139.Anderson, T.H., Silver, L.T., 2005, The Mojave-Sonora megashear – field and analytical studies leading to the conception and evolution of the hypothesis, *in* Anderson, T.H., Nourse, J.A., McKee, J.W., Steiner, M.B. (eds.), The Mojave-Sonora Megashear Hypothesis: Development, Assessment, and Alternatives: Boulder, Colorado, Geological Society of America, Special Paper 393, 1-50.

Anderson, T.H., Silver, L.T., Salas, G.A., 1980, Distribution and U-Pb isotope ages of some lineated plutons, northwestern Mexico: Geological Society of America, 153, 269-283.

Avigad, D., Kolodner, K., McWilliams, M., Persing, H., Weissbrod, T., 2003, Origin of northern Gondwana Cambrian sandstone revealed by detrital zircon SHRIMP dating: Geology, 31(3), 227-230.

Campa, M.F., Coney, P., 1983, Tectono-stratigraphic terranes and mineral resource distributions of Mexico: Canadian Journal of Earth Sciences, 20, 1040-1051.

Baldridge, W.S., 2004, Geology of the American Southwest: Cambridge, Cambridge University Press, 280 pp.

Barbeau, D.L.Jr., Ducea, M.N., Gehrels, G.E., Kidder, S., Wetmore, P.H., Saleeby, J.B., 2005, U-Pb detrital-zircon geochronology of northern Salinian basement and cover rocks: Geological Society of America Bulletin, 117(3-4), 466-481.

Bhattacharya, A., Mohanty, L., Maji, A., Sen, S.K., Raith, M., 1992, Non-ideal mixing in the phlogopite-annite binary: constraints from experimental data on Mg-Fe partitioning and a reformulation of the biotite-garnet thermometer: Contributions to Mineralogy and Petrology, 111(1), 87-93.

Burchfiel, B.C., Cowan, D.S., Davis, G.A., 1992, Tectonic overview of the Cordilleran orogen in the western United States, *in* Burchfiel, B.C., Lipman, P.W., Zoback, M.L. (eds.), The Cordilleran Orogen: Conterminous U.S: Boulder, Colorado, Geological Society of North America, 407-479.

Damon, P.E., Shafiqullah, M., Roldán-Quintana, J., Cochemé, J.J., 1983, El batolito Laramide (90-40 Ma) de Sonora: Guadalajara, Asociación de Ingenieros de Minas, Metalurgistas y Geólogos de México (AIMMGM), Memoria Técnica 15, 63-95.

De Cserna, Z., Kent B.H., 1961, Mapa geológico de reconocimiento y secciones estructurales de la región de San Blas y El Fuerte, Estado de Sinaloa, Cartas Geológicas y Mineras No. 4, Instituto de Geología, UNAM, escala 1:100,000.

Farmer, G.L., Bowring, S.A., Espinosa-Maldonado, G., Fedo, C., Wooden, J., 2005, Paleoproterozoic Mojave province in northwestern Mexico? Isotopic and U-Pb zircon geochronologic studies of Precambrian and Cambrian crystalline and sedimentary rocks, Caborca, Sonora, *in* Anderson, T.H., Nourse, J.A., McKee, J.W., Steiner, M.B. (eds.), The Mojave-Sonora Megashear Hypothesis: Development, Assessment, and Alternatives: Boulder, Colorado, Geological Society of America, Special Paper 393, 183-198.

Gehrels, G.E., Dickinson, W.R., Ross, G.M, Stewart, J.H., Howell,

D.A., 1995, Detrital zircon reference for Cambrian to Triassic miogeoclinal strata of western North America: Geology, 23(9), 831-834.

Gehrels, G.E., Dickinson, W.R., Riley, B.C.D., Finney, S.C., Smith, M.T., 2000, Detrital zircon geochronology of the Roberts Mountains Allochthon, Nevada, *in* Soreghan, M.J., and Gehrels, G. (eds.), Paleozoic and Triassic paleogeography and tectonics of western Nevada and Northern California: Boulder, Colorado, Geological Society of America, Special Paper 347, 19-42.

Gehrels, G.E., DeCelles, P.G., Ojha, T.P., Upreti B.N., 2006, Geologic and U-Th-Pb geochronologic evidence for early Paleozoic tectonism in the Kathmandu thrust sheet, central Nepal Himalaya: Geological Society of America Bulletin, 118(1-2) 185-198.

Gillis, R.J., Gehrels, G.E., Ruiz, J., Flores de Dios, L.A., 2005, Detrital zircon provenance of Cambrian–Ordovician and Carboniferous strata of the Oaxaca terrane, southern Mexico: Sedimentary Geology, 182(1-4), 87-100.

Graham, C.M., Powell, R., 1984, A garnet-hornblende geothermometer: calibration, testing, and application to the Pelona Schist, Southern California: Journal of Metamorphic Geology, 2(1), 13-31.

Gross, E.L., Stewart, J.H., Gehrels, G.E., 2000, Detrital zircon geochronology of Neoproterozoic to Middle Cambrian miogeoclinal and platformal strata: northwest Sonora, Mexico: Geofísica Internacional, 39(4), 295-308.

Holdaway, M.J., 1971, Stability of andalusite and the aluminum silicate phase diagram: American Journal of Science, 271, 97-131.

Hynes, A., Forest, R.C., 1988, Empirical garnet–muscovite geothermometry in low-grade metapelites, Selwyn Range (Canadian Rockies): Journal of Metamorphic Geology, 6(3), 29-309.

Keppie, D.J., Dostal, J., Miller, B.V., Ortega-Rivera, A., Roldán-Quintana, J., Lee, J.W.K., 2006, Geochronology and geochemistry of the Francisco Gneiss: Triassic continental rift tholeiites on the Mexican margin of Pangea metamorphosed and exhumed in a Tertiary core complex: International Geology Review, 48(1), 1-16.

Kohn, M.J., Spear, F.S., 1989, Empirical calibration of geobarometers for the assemblage garnet + hornblende + plagioclase + quartz: American Mineralogist, 74, 77-84.

Ludwig, K.R., 2003, User´s Manual for Isoplot 3.00. A Geochronological Toolkit for Microsoft Excel: Berkeley, California, Berkeley Geochronology Center, Special Publication 4.

Massonne, H.J., Schreyer, W., 1987, Phengite geobarometry based on the limiting assemblage with K-feldspar, phlogopite, and quartz: Contributions to Mineralogy and Petrology, 96, 212-224.

Mullan, H.S., 1978, Evolution of the Nevadan orogen in northwestern Mexico: Geological Society of America Bulletin, 89(8), 1175-1188.

Poole, F.G., Madrid, R.J., 1988, Allochthonous Paleozoic eugeoclinal rocks of the Barita de Sonora mine area, central Sonora, Mexico, *in* Rodríguez-Torres, R. (ed.), El Paleozoico de la región central del Estado de Sonora, Libreto Guía de la Excursión para el Segundo Simposio sobre la Geología y Minería en el Estado de Sonora: Sonora, Instituto de Geología, Universidad Nacional Autónoma de México, 32-41.

Poole, F.G., Perry, W.J. Jr., Madrid, R.J., Amaya-Martínez, R., 2005, Tectonic synthesis of the Ouachita-Marathon-Sonora orogenic margin of southern Laurentia: Stratigraphic and structural implications for timing of deformational events and plate-tectonic model, *in* Anderson, T.H., Nourse, J.A., McKee, J.W., Steiner, M.B. (eds.), The Mojave-Sonora Megashear Hypothesis: Development, Assessment, and Alternatives: Boulder, Colorado, Geological Society of America, Special Paper 393, 543-596.

Passchier, C. W., Trouw, R.A.J., 1996, Microtectonics: Berlin, Heidelberg, Springer, 289 pp.

Riley, B.C.D., Snyder W.S., Gehrels, G.E., 2000, U-Pb detrital zircon geochronology of the Golconda allochthon, Nevada, *in* Gehrels, G.E., Meghan, M. (eds.), Detrital zircon geochronologic study of upper Paleozoic strata in the eastern Klamath terrane, northern California: Boulder, Colorado, Geological Society of America, Special, Paper 347, 65-75.

Salgado-Souto, S.A., 2006, Petrología, termobarometría y geocronología del Grupo Río Fuerte, región de El Fuerte, Sinaloa: Hermosillo, Sonora, Departamento de Geología, Universidad de Sonora, tesis de maestría, 121 pp.

Sedlock, R.L., 2003, Four phases of Mesozoic deformation in the Sierra de San Andrés ophiolite, Vizcaíno Peninsula, west-central Baja California, México, *in* Johnson, S.E., Paterson, S.R., Fletcher, J.M., Girty, G.H., Kimbrough, D.L., Martín-Barajas, A. (eds.), Tectonic evolution of Northwestern México and the Southwestern USA: Boulder, Colorado, Geological Society of America, Special Paper 374, 73-92.

Sedlock, R.L., Ortega-Gutiérrez, F., Speed, R.C., 1993, Tectonostratigraphic Terranes and Tectonic Evolution of Mexico: Boulder, Colorado, Geological Society of America Special Paper 278, 153 pp.

Schweickert, R.A., Bogen, N.H., Girty, G.H., Hanson, R.E., Merguerian, C., 1984, Timing and structural expression of the Nevadan orogeny, Sierra Nevada, California: Geological Society of America Bulletin, 95(8), 967-979.

Shannon, W.M., Barnes, C.G., Bickford, M.E., 1997, Grenville Magmatism in West Texas: Petrology and Geochemistry of the Red Bluff Granitic Suite: Journal of Petrology, 38(10) 1279-1305.

Spear, F.S., 1995, Metamorphic phase equilibria and pressure-temperature-time paths: Chelsea, Mineralogical Society of America Monograph, 799 pp.

Stewart, J.H., 2005, Evidence for Mojave-Sonora megashear-Systematic left-lateral offset of Neoproterozoic to Lower Jurassic strata and facies, western United States and northwestern Mexico, *in* Anderson, T.H., Nourse, J.A., McKee, J.W., Steiner, M.B. (eds.), The Mojave-Sonora Megashear Hypothesis: Development, Assessment, and Alternatives: Boulder, Colorado, Geological Society of America, Special Paper 393, 209-232.

Stewart, J.H., Gehrels, G., Barth, A.P., Link, P.K., Christie-Blick, N., Wrucke, C.T., 2001, Detrital zircon provenance of Mesoproterozoic to Cambrian arenites in the western United States and northwestern Mexico: Geological Society of America Bulletin, 113(10) 1343-1356.

Talavera-Mendoza, O., Ruiz, J., Gehrels, G.E., Meza-Figueroa, D., Vega-Granillo, R., Campa-Uranga, M.F., 2005, U-Pb geochronology of the Acatlán Complex and implications for the Paleozoic paleogeography and tectonic evolution of southern Mexico: Earth and Planetary Science Letters, 235(3-4) 682-699.

Valencia, V.A., Ruiz, J., Barra, F., Gehrels, G., Ducea, M., Titley, S.M., Ochoa-Landin, L., 2005, U-Pb single zircon and Re-Os geochronology from La Caridad Porphyry Copper Deposit: Insights for the duration of magmatism and mineralization in the Nacozari District, Sonora, Mexico: Mineralium Deposita, 40, 175-191.

Vega-Granillo, R., Talavera-Mendoza, O., Meza-Figueroa, D., Ruiz, J., Gehrels, G., López Martínez, M., de la Cruz Vargas, J.C., 2007, Pressure-temperature-time evolution of Paleozoic high-pressure rocks of the Acatlán Complex (southern Mexico): implications for the evolution of the Iapetus and Rheic Oceans: Geological Society of America Bulletin, 119(9-10), 1249-1264.

Vega-Granillo, R., Salgado-Souto, S., Herrera-Urbina, S., Valencia, V., Ruiz, J., Meza-Figueroa, D., Talavera-Mendoza, O., 2008, U-Pb detrital zircon data of the Rio Fuerte Formation (NW Mexico): its peri-Gondwanan provenance and exotic nature in relation to southwestern North America: Journal of South American Earth Sciences, 26(4), 343-354.

Vega-Granillo, R., Calmus, T., Meza-Figueroa, D., Ruiz, J., Talavera-Mendoza, O., López-Martínez, M., 2009, Structural and tectonic evolution of the Acatlán Complex, southern Mexico: its role in the collisional history of Laurentia and Gondwana: Tectonics, 28, 1-25.

Manuscript received: June 9, 2010
Corrected manuscript received: November 4, 2010
Manuscript accepted: November 22, 2010